Grain growth on reheating for an as-cast Al-Nb-containing steel with segregated composition

Fei **Wang** [*a, c], Claire **Davis** [b] and Martin **Strangwood** [a]

[a] *Department of Metallurgy and Materials, University of Birmingham, Edgbaston, Birmingham, B15 2TT, UK*

[b] *Warwick Manufacturing Group, University of Warwick, Coventry, CV4 7AL, UK*

[c] *State Key Laboratory of Advanced Stainless Steel, TISCO, Taiyuan, 030003, China*

*Corresponding author

E-mail addresses:

Fei Wang, feistime@hotmail.com

Claire Davis, Claire.Davis@warwick.ac.uk

Martin Strangwood, m.strangwood@bham.ac.uk

Grain growth on reheating for an as-cast Al-Nb-containing steel with segregated composition

Abstract

Reheating treatments for as-cast Al-Nb-containing steel were examined at temperatures correlating to the predicted dissolution temperatures of the precipitates present in the interdendritic and dendritic regions. Bimodal grain growth was observed in this steel when reheated in the range 1160 – 1200 ºC as Nb-rich particles remaining in the interdendritic region prevented further growth of grains originating from dendritic region when the pinning precipitates of AlN dissolved. The isolated abnormally large grain structure seen for the homogenised condition from previous work was not observed in the as-cast Al-Nb steel under any conditions. It is suggested that elemental segregation (particularly for Nb) plays a role in providing a spatially distributed (banded) pinning effect on the large grains growing from the dendritic regions.

Key words: As-cast steel, Segregation, Reheating treatment, Abnormal grain growth, Bimodal grain growth.

Introduction

Grain size plays a key role in controlling the strength and toughness in steel and a uniform size distribution after reheating is desired to ensure even refinement, and hence generation of a uniform fine size in the final product, during hot deformation. Grain size control is achieved in high strength low alloy steel (HSLA) steels (which are low carbon steels with minor additions of microalloying elements, such as Nb, Ti and V) because the microalloying precipitates provide a pinning force resisting the movement of grain boundaries and so restricting grain growth during casting, reheating treatment and thermo-mechanically controlled rolling (TMCR) [1-5]. However, undesired non-uniform grain structures, such as from abnormal grain

growth (AGG) and bimodal grain growth (BGG) can occur during reheating, which can then result in a non-uniform final recrystallised grain size and increased scatter in mechanical properties [6-11].

Bimodal grain size development is identified as non-uniform distributed structures consisting of alternate large-grained and small-grained regions, which has been linked to the inhomogeneous precipitate distribution in segregated steel [12-16]. Micro-segregation occurs during solidification, where the local compositions vary between the solid and liquid regions over a distance corresponding to the secondary dendrite arm spacing (SDAS), resulting in interdendritic solute-enriched regions and dendritic solute-depleted regions. Most alloying elements, such as Nb, Ti, V, and Mn prefer to partition into the interdendritic liquid, while Al has been reported to slightly partition to the dendritic solid regions during solidification [17]. Due to the slow diffusion of elements (especially for substitutional elements) the interdendritic regions, with higher Nb, can be precipitate-rich regions in the solidified state compared with dendritic regions[18]. An inhomogenous pinning force is therefore expected during reheating especially when precipitates dissolve in the solute-depleted dendritic regions but are still present in the solute-enriched interdendritic regions, and this can result in non-uniform grain growth such that bands of coarse and fine grains are observed.

Abnormal grain growth, resulting in isolated large grains surrounded by small grains, has been reported by many researchers[10, 19-27] as being due to the local unpinning of grain boundaries associated with dissolution of microalloying precipitates. Abnormally large grains have been reported to be defined by the relative difference (*RD*) between the large grain(s) size and the mean size of the normal grains, where abnormal grain growth is when *RD* exceeds 0.9 [28]; or when the abnormally

large grains are approximately 2 times compared to the normal grain size [29, 30]. The reports of AGG have been for studies on homogenised or rolled plate material (where any inhomogeneity in composition due to segregation will be over distances similar to or less than the initial grain size on reheating due to the reduction in thickness during rolling). Reports on BGG have been for steels in an as-cast condition. No reports have considered homogenised and as-cast material of the same composition to examine the role of segregation on conditions under which AGG or BGG can occur.

Previous work [31] has investigated grain growth in a homogenised Al-Nb-containing steel where abnormally large grains were observed on reheating to 1170 ºC, corresponding to the calculated dissolution temperature of AlN, which was the most stable precipitate present (note that Nb(C,N) precipitates were also present but with a lower dissolution temperature (1090 ºC) than the AlN in this steel). In this paper austenite grain growth behaviour during reheating treatment of the corresponding as-cast Al-Nb-containing HSLA steel has been examined to determine if abnormal or bimodal grain size distributions can be generated. In particular the effect of a segregated composition on grain size development in steel that has been shown to display AGG in the homogenised condition is reported.

Experimental

A sample from a 60 kg laboratory as-cast ingot of Al-Nb containing HSLA steel (chemical composition shown in Table 1) measuring 340 mm long with a 130 × 130 mm cross-section was supplied by Tata Steel, UK. The precise cooling history was not available, but was inferred from the dendritic structure.

Table 1 Chemical composition (wt %) of the as-cast Al-Nb containing HSLA steel

C	Si	Mn	P	S	Cr	Mo	Ni	Al	N	Nb	Ti	V
0.1	0.29	1.42	0.018	0.004	0.01	0.005	0.32	0.057	0.008	0.019	0.001	0.052

Samples measuring 10 × 15 × 20 mm were machined from the quarter position (quarter width and depth) of the as-cast Al-Nb ingot well away from the top and base. Reheating trials with a heating rate of 3.8 ºC/s (measured by a K-type thermocouple attached to the sample) were carried out for one hour at temperatures in the range from 925 ºC to 1300 ºC, Figure 1, covering the precipitate dissolution temperatures for the segregated compositions predicted by Thermo-Calc (as will be discussed in next section). All reheated samples were quenched to give martensite then tempered at 550 ºC for 6 hours as this was found to reveal the prior austenite grain boundaries clearly on etching in hot (60 ºC) saturated picric acid (20g picric acid, 1000 ml H_2O, 14 drops HCl and 5 ml TEEPOL). Metallographic samples were sectioned along the primary dendrite growth direction (from the known solidification directions in the original ingot) then mounted in Bakelite. All the samples were ground and polished to a 1µm MD-Nap diamond finish and etched in 2%-nital (2 ml HNO_3 in 98 ml ethanol) to reveal the initial microstructure or in hot saturated aqueous picric acid with magnetic stirring, to reveal the prior austenite grain structure.

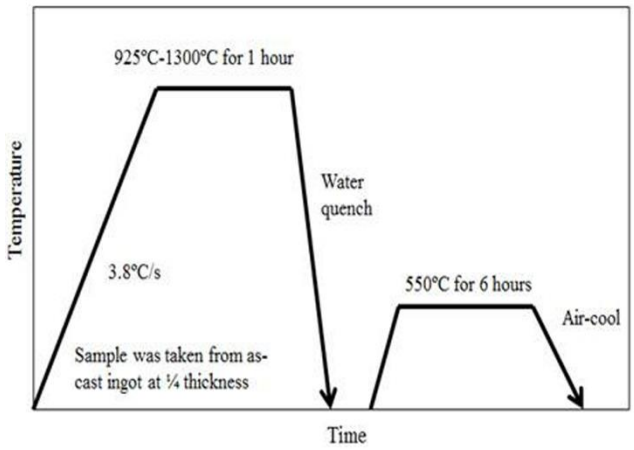

Figure 1 Reheating schedule of as-cast Al-Nb ingot samples for 1 hour.

The samples were characterised using a Zeiss Axioskop-2 optical microscope equipped with AxioVison image capture software. The proportion of pearlite in the ferritic and pearlitic microstructure was analysed by ImageJ software (windows version), and the prior-austenite grain size (measured manually on at least 1000 grains per sample as an ECD (equivalent circle diameter) value) in the martensitic structure. The grain size distributions were established to characterise the different grain growth behaviour as a function of reheating temperature.

Microalloying precipitates in the as-cast samples were characterised by using a JEOL 7000 scanning electron microscope (SEM) operating at 20 kV with field emission gun (FEG), and the particle compositions were analysed using an Oxford INCA energy dispersive X-ray spectroscopy (EDS) system, conducted at 10 mm working distance. Moreover, secondary-electron (SE) imaging for morphology analysis and back-scattered electron (BSE) imaging for compositional contrast (due to different atomic numbers) were used to distinguish Al-rich (generally dark) and Nb-rich (normally bright) particles in the as-cast and reheated samples.

As noted above, segregation of microalloying elements has been associated with inhomogeneous grain distributions, but reliable measurement of segregation profiles

for these elements (Nb and Al in this steel) at such low contents are difficult to obtain from 2D sections. This is still the case if techniques, such as cumulative profile based on ranking data from EDS grid-mapping are used. Hence, the general segregation behaviour was determined using profile ranking for [Mn], the concentration of which is sufficiently large to measure using SEM-EDS, as Mn is known to segregate to the interdendritic regions[32]. A grid of around 300 SEM-EDS point spectra arranged in a square pattern with a spacing greater than half the SDAS value (75 μm) was taken and ranked from lowest (dendrite centre) to highest (centre of interdendritic region) Mn concentrations. The resulting profile for [Mn] was then compared with DICTRA-predicted profiles (using TC-Fe7 and MobFe2 database) for the Fe-C-Mn-Nb-Al system to estimate the segregation profiles for Nb and Al.

Results and discussions

Initial microstructure characterisation for as-cast Al-Nb containing steel

In order to investigate the role of segregation during solidification on the grain size development after reheating, the spatial separation of the segregated regions needs to be determined. The initial microstructure of as-cast steel is shown in Figure 2, consisting of pearlite (area fraction of around 18%) and ferrite where pearlite forms in the interdendritic regions allowing the original as-cast dendritic morphology to be revealed. The average secondary dendrite arm spacing (SDAS) was measured as 150 $\pm$50 μm for the 1/4 thickness position of the as-cast Al-Nb containing ingot, and the solidification rate (C_R) estimated for this SDAS and steel composition was 0.4 ºC/s according to equation 1, for a low carbon steel (% C $\leqslant$ 0.15 wt %) [33].

$$\lambda_{SDAS} = \left(169.1 - 720.9(\%\ C)\right) \times C_R^{-0.4935} \qquad (1)$$

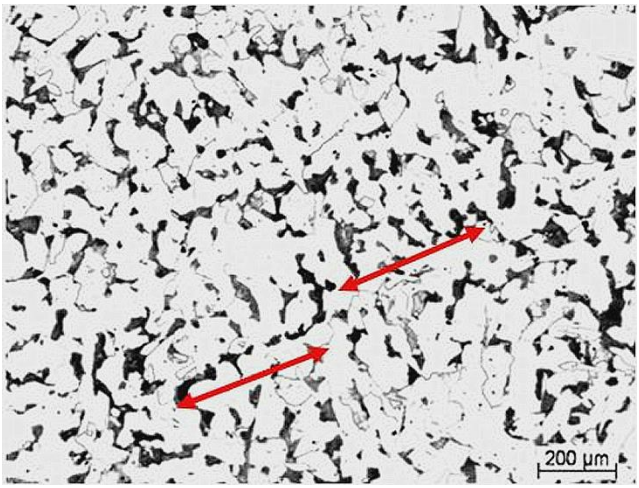

Figure 2 Microstructure of the as-cast Al-Nb ingot at the 1/4 position, consisting of bright ferrite and dark pearlite; the dendritic structure can be clearly seen, examples where the measured secondary dendrite arm spacing are arrowed.

As expected, Mn segregated to the pearlitic regions (characterised by EDS analysis) with values up to 1.8 wt% recorded, whilst concentrations down to 1 wt% were recorded from point analyses in the dendritic ferrite regions, Figure 3(a); the ranked [Mn] profile is given in Figure 3(b).

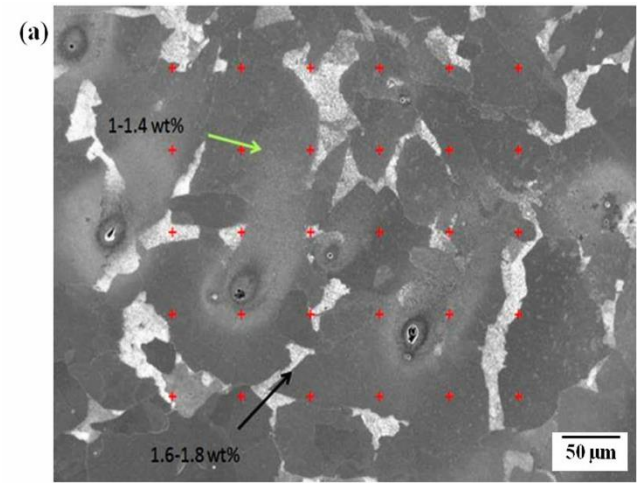

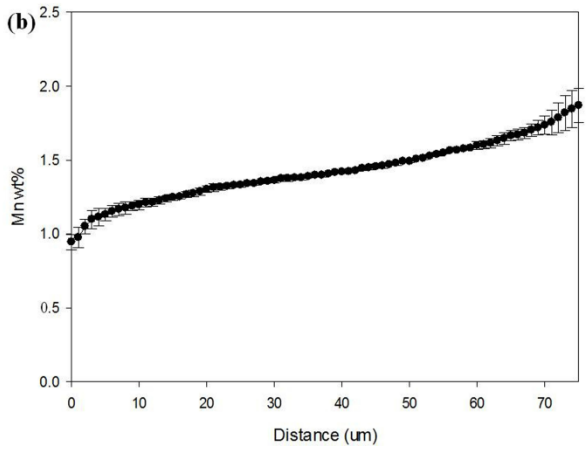

Figure 3 Grid analysis points located over both dendritic ferritic (dark region) and interdendritic pearlitic (light grey region) areas in the as-cast microstructure under SEI imaging; (b) Mn content against the distance of half SDAS.

DICTRA was used, as verified in previous studies[34, 35] to predict the microsegregation behaviour of elements (e.g. Mn and Si) during solidification and cooling, including the influence of any solid-state phase transformation. No significant changes in [Mn] profile are expected at temperatures below the eutectoid temperature, so that the simulated profile of Mn at 780 ºC was calculated and compared to the experimental concentration profile, Figure 4. The predicted composition profile is generally consistent with the measured experimental results, although the DICTRA prediction is generally flatter than the experimental one except at the dendrite centre, which may indicate that the cooling rate used in the simulation is too low and more back diffusion occurs from the enriched interdendritic region in the prediction than actually occurs in practice. However, the generally good agreement between composition profiles means that DICTRA can be used to describe the microsegregation behaviour of Mn, and therefore, it is also expected to be applicable to other elements in the Al-Nb steel. Unlike Mn, however, Al and Nb would be expected to precipitate (as nitrides and carbo-nitrides respectively) during

cooling, especially in segregated regions (as will be discussed in the next section) where any effective solubility limit will be more readily exceeded.

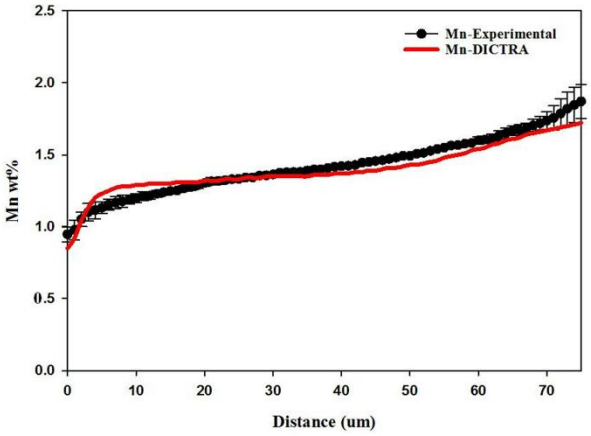

Figure 4 Comparison between the experimental concentration profile of Mn and the DICTRA prediction of Mn composition profile after solidification and cooling to 780 ºC after the austenite to ferrite transformation.

SEM examination of the as-cast ingot confirms precipitation of microalloy-rich particles. Al-rich particles, expected to be AlN with irregular shapes (facetted and rounded shapes), have been mainly observed in the ferrite regions, as shown in Figure 5 (a-c). Spherical Nb-rich particles (expected to be Nb(C,N)) have been observed in the interdendritic areas and on ferrite boundaries in the as-cast structure, Figure 5 (d-f).

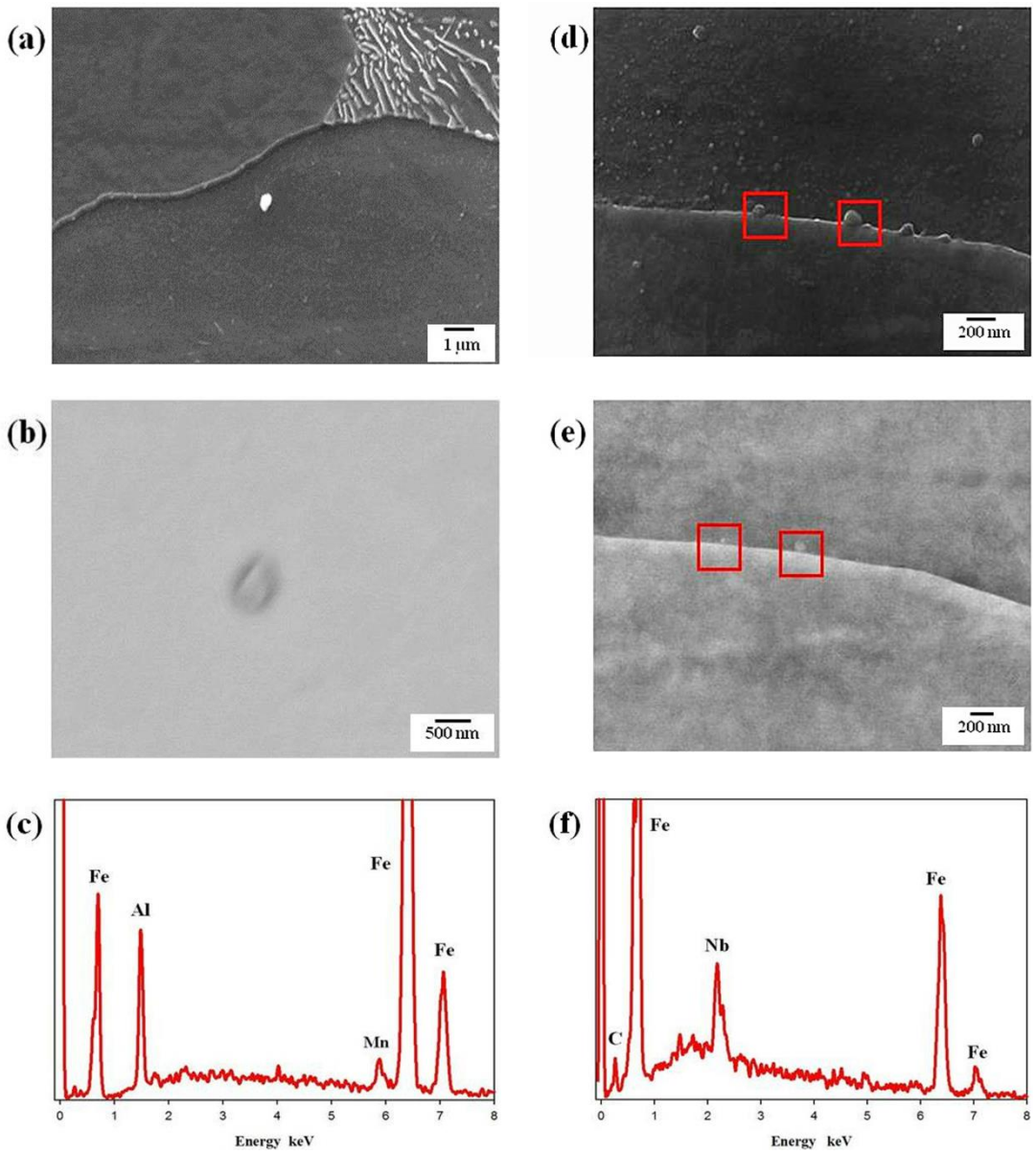

Figure 5 Characterisation of precipitates for Al-rich particle: (a) SE image; (b) BSE image where the AlN particle appears dark due to its lower atomic weight than iron; and (c) EDS trace indicating the Al peak; and for Nb-rich particle: (d) SE image; (e) BSE image where the Nb-rich particle appears light due to its higher atomic weight than iron; and (f) EDS trace showing the Nb peak.

The majority of the ferrite present in the as-cast steel represents prior dendritic regions and the precipitate distributions for solute-depleted material were characterised from these. The solute-enriched, interdendritic regions largely transformed to pearlite on cooling so that the corresponding precipitate distributions were characterised from these. However, the carbide plate structure of pearlite hampered identification and measurement of the finer alloy carbo-nitrides so that

some idiomorphic ferrite islands (surrounded by pearlite microstructure) in the pearlitic region, as shown in Figure 6 (a), were also investigated to characterise the particle distributions in the solute-enriched region, as was reported by Zheng [17] for a similar steel. For example, a cluster of Nb-rich particles from an idiomorphic ferrite island is shown in Figure 6 (b), with a confirmatory EDS spectrum in Figure 6 (c).

The distribution of Al-rich and Nb-rich precipitates in the dendritic and interdendritic regions was analysed by Kundu in same material [36], Figure 7, indicating that there is a much higher number density of Nb-rich particles in the interdendritic region than in the dendritic region, which is due to the strong segregation of Nb into the interdendritic area. The number density of Al-rich particles, however, does not show a large difference between the two regions with slightly more precipitates appearing in the dendritic solute-depleted region. The precipitation behaviour of AlN and Nb(C,N) in the homogenised [31] and as-cast samples are compared in Table 2, indicating that the elemental segregation has not caused a significant change in the particles size but has resulted in a marked spatially heterogeneous distribution of particles in the matrix, i.e. the number density is significantly different in the dendritic and interdendritic regions where the total number density of interdendritic particles ($3.93 \times 10^4/mm^2$) is approximately one and a half times greater than that in the dendritic region ($2.62 \times 10^4/mm^2$).

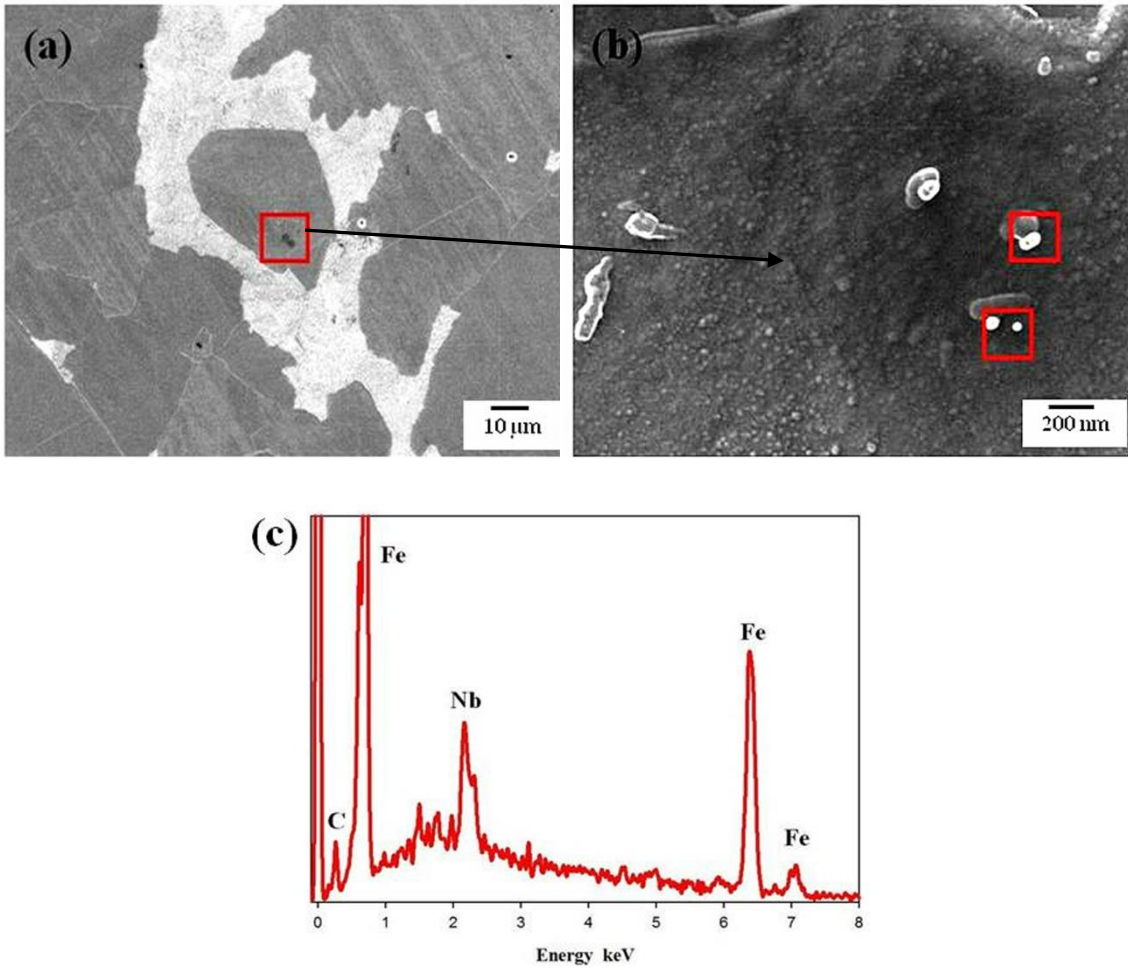

Figure 6 (a) Isolated ferrite located in the pearlite region; (b) Nb-rich particles distributed within this region; (c) EDS trace indicating the Nb peak.

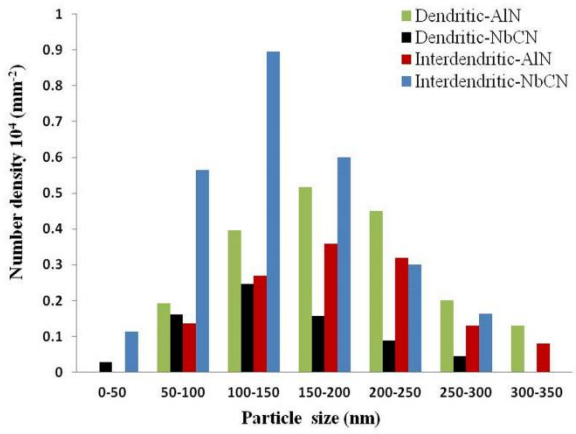

Figure 7 Distribution of Al-rich and Nb-rich precipitates size with number density in the dendritic and interdendritic regions for the as-cast Al-Nb containing steel was analysed by Kundul [36].

Table 2 Precipitation behaviour of AlN and Nb(C,N) in the homogenised [31] and as-cast samples.

	Homogenised [31]		Dendritic solute-poor		Interdendritic solute-rich	
	AlN	Nb(C,N)	AlN	Nb(C,N)	AlN	Nb(C,N)
Mode size, nm	150-200	150-200	150-200	100-150	150-200	100-150
Number density, $\times 10^4/mm^2$	1.12	0.81	1.89	0.73	1.29	2.64

Thermo-Calc prediction of microalloying precipitates' thermal-stability

The stability of precipitates in the as-cast sample can be determined by Thermo-Calc using the simulated composition profile from DICTRA for the dendritic and interdendritic regions. As Al and Nb form precipitates at high temperatures the composition profile predicted by DICTRA at 1476 ºC, close to the solidus temperature (about 1480 ºC predicted by Thermo-Calc), has been considered. Solidification occurs as delta ferrite initially followed by austenite, therefore different profiles due to the different partition ratios between the liquid and delta ferrite and liquid and austenite result, with the final liquid being heavily enriched in Nb or depleted in Al, Figure 8. The concentration steps observed in the Nb and Al composition profiles at a distance of around 15 μm from the left-hand side of the graph (as seen in Figure 8), due to the lower partition behaviour at the interface of liquid/austenite than that in the liquid/ferrite will disappear after complete transformation from δ-ferrite to austenite, as elemental redistribution occurs during phase transformation at the moving ferrite-austenite interface.

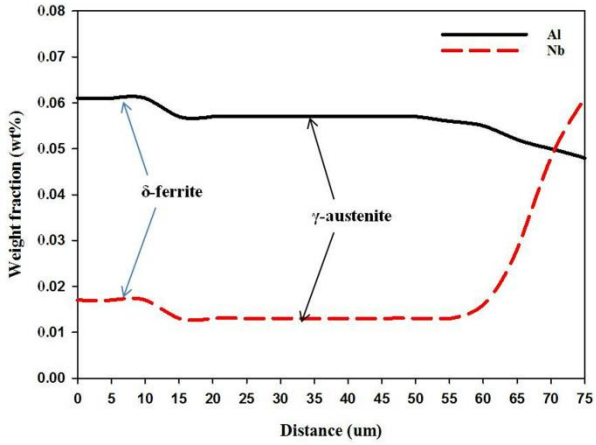

Figure 8 Composition profile of Al and Nb over the distance of half SDAS (from dendrite centre towards interdendrite centre) predicted by DICTRA after solidification at a temperature of 1476 ºC.

The input compositions of Al and Nb for the Thermo-Calc calculation of precipitate stability in the interdendritic and dendritic regions were taken from the right-hand side (75 µm) and left-hand side (0 µm) from the composition profile in Figure 8 respectively, while other elements were assumed to be the average composition in the steel due to their fast diffusion behaviour (e.g. C and N) or their insignificant partition behaviour during casting (e.g. V). The predicted precipitate dissolution temperatures in the as-cast sample are shown in Figure 9 (a) along with the volume fractions against temperature for AlN and Nb(C,N) in the different regions. A simple schematic diagram in Figure 9 (b) indicates the dissolution behaviour of Nb(C,N) and AlN from the dendritic and interdendritic regions in a half SDAS space with increasing reheat temperature, which can be used to understand the expected grain growth behaviour corresponding to the unpinning effect in these regions, discussed below. The predicted volume fraction for AlN and Nb(C,N) is generally consistent with the measured results, as summarised in Table 3, although the volume fraction of AlN measured in the homogenised sample is lower than predicted [31]; this may be due to some AlN particles being missed in the SEM characterization as the pearlite is

uniformly distributed and makes full quantification more difficult, which is supported with evidence that the measured number density of AlN in the homogenised material ($1.12 \times 10^4/mm^2$) is lower than the number density of AlN in the as-cast samples (e.g. $1.89 \times 10^4/mm^2$ in the dendritic region and $1.29 \times 10^4/mm^2$ in the interdendritic region). The predicted results in the interdendritic solute-rich region are higher than measured for both AlN and Nb(C,N) in the as-cast steel, which may be due to the compositions from DICTRA being too high as these were taken from a temperature close to the solidus whereas some back diffusion is expected on cooling before precipitation occurs.

Previous work [31] has found that dissolution of the predominant grain boundary pinning precipitates (e.g. AlN, which dissolved at 1170 ºC) in the homogenised sample resulted in abnormally grain growth. This suggests that grain growth will occur in the dendritic area at temperatures above 1160 ºC in the as-cast sample, when the dissolution of the predominant pinning particles, dendritic AlN, takes place (at 1160 ºC). However, pinning particles (Nb(C,N)) are expected to remain in the interdendritic region until 1230 ºC. Reheating trials in the temperature region of 1160 - 1230 ºC were conducted to determine whether the undissolved interdendritic Nb(C,N) provide an effective pinning force on the boundaries of growing grains originating from the dendritic region.

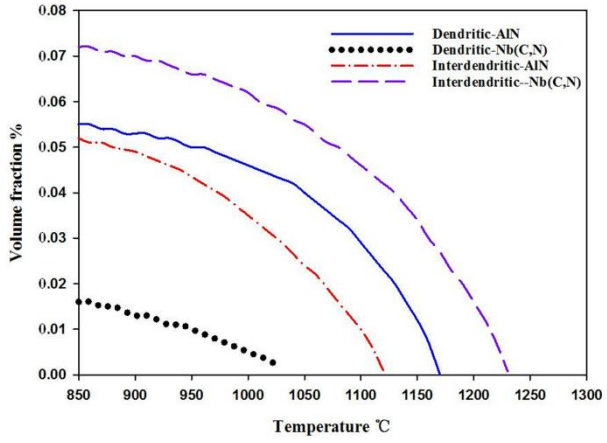

(a)

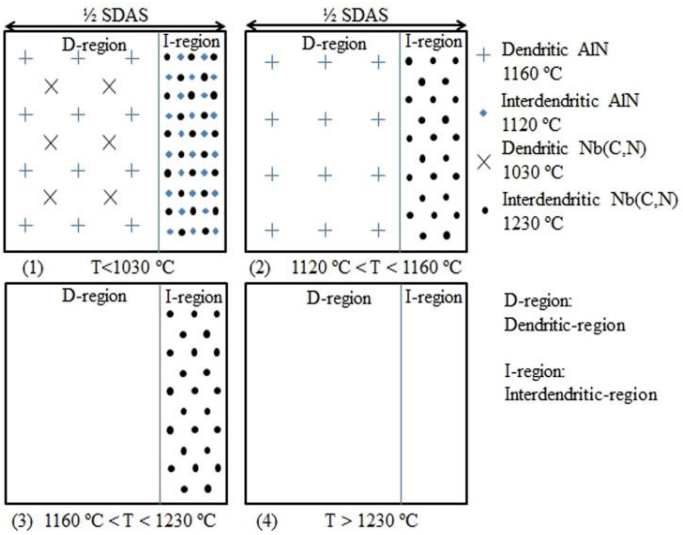

(b)

Figure 9 (a) Predicted dissolution temperature of precipitates for the as-cast segregated sample; (b) schematic diagrams to illustrate the precipitates' dissolution behaviours in the dendritic and interdendritic regions of a half SDAS space with different holding temperatures covering the predicted dissolution temperature from Thermo-Calc.

Table 3 Comparison between experimental precipitate volume fractions and modelling predictions for AlN and Nb(C,N) in the homogenised [31] and as-cast samples.

	Experimental result, %	Modelling prediction, %
Homogenised-AlN [31]	0.040	0.055
Homogenised-Nb(C,N) [31]	0.020	0.023
As-cast dendritic-AlN	0.059	0.055
As-cast dendritic-Nb(C,N)	0.014	0.016
As-cast interdendritic-AlN	0.040	0.052
As-cast interdendritic-Nb(C,N)	0.050	0.072

Grain growth in as-cast Al-Nb containing steel with microsegregation

As-cast samples were reheated in the temperature range from 925 ºC to 1300 ºC, and the prior austenite grain sizes were examined and plotted using mode grain size and 95% grain size (the extreme of grain size in the accumulated area fraction with size distribution), as shown in Figure 10(a). The predicted volume fractions of dendritic and interdendritic precipitates with temperature are shown in Figure 10(b).

No grain growth was observed on reheating for one hour in the temperature range of 925 ºC – 1130 ºC, with a stable mode grain size of approximately of 30 μm being observed, indicating that the dissolution of dendritic Nb-rich particles (dissolution temperature of 1030 ºC) and interdendritic Al-rich precipitates (dissolution temperature of 1120 ºC) does not result in any grain growth as undissolved precipitates in the dendritic (AlN with volume fraction: 0.02%, Figure 10(b)) and interdendritic regions (Nb(C,N) with volume fraction: 0.04%, Figure 10(b)) are still effective in pinning grain boundaries. Previous work found that a predicted volume fraction of AlN at 1150 ºC (0.01%) was still effective at pinning grain boundaries and

preventing grain growth in the homogenised sample [31]. The fine and uniform grain structure at 1130 ºC is shown in Figure 11 (a-b).

Due to the dissolution of the pinning dendritic AlN precipitates at 1160 ºC (as shown in Figure 10(b)), grain growth was observed when reheating at 1160 ºC for 1 hour, where the mode grain size increased from around 30 µm for reheating temperatures < 1150 ºC to approximately 75 µm at 1160 ºC; and the 95% area fraction grain size also increased significantly from approximately 45 – 65 µm (<1150 ºC) to 195 µm at 1160 ºC. An obvious bimodal microstructure was observed on reheating in the temperature range where dendritic AlN dissolved but interdendritic Nb(C,N) remained with a banded structure consisting of alternating regions of small and large grains being shown at 1160 ºC, Figure 11(c-d), and 1200 ºC, Figure 11 (e-f). The grain size distributions indicated two distributions with separate mode grain sizes (75 µm and 135 µm, arrowed in Figure 11(d)) corresponding to the bands of small and large grains respectively. When reheating at 1200 ºC, two mode grain sizes are still observed in the grain size distribution, as shown in Figure 11(f), where an increase in the large mode grain size (185 µm) occurs compared to that at 1160 ºC (135 µm). This suggests that grains in the dendritic solute-depleted regions are growing larger at the higher reheat temperature as pinning force reduces (more dendritic AlN has dissolved) and the driving force for grain growth increases. However, as noted earlier a nearly stable 95% large grain size was observed at 1160 ºC (195 µm) and 1200 ºC (205 µm), which indicates that boundary pinning in the solute-enriched band provided by interdendritic Nb-rich particles (approximately 0.02% volume fraction, Figure 10(b)) is still able to limit the growing dendritic large grains to restrict their size to within the maximum distance of the SDAS, resulting in no grain growth in temperature range of 1160 ºC-1200 ºC, Figure 10(a). This means that

an abnormally large grain structure (markedly large isolated grains surrounded by small grains, as found in the previous study [31], where isolated grains as large as 290 μm were observed) does not occur at these temperatures. It is interesting to note that, the size ratio of the largest grains to the small grain mode size for the bimodal distribution is around 2.6 which is greater than the published criteria of "2" for the determination of abnormal grain growth, but less than observed for the homogenised samples where a ratio of 6-7 was seen [31]. However, as these are not isolated abnormally large grains but bands of coarse grains it is not a typical abnormal grain-structure and is therefore termed a bimodal distribution.

Reheating in the temperature range of 1230 ºC – 1300 ºC resulted in significant growth as shown in Figure 10(a), which indicates that the interdendritic pinning force was ineffective (presumably due to the dissolution of interdendritic Nb(C,N) starting at around 1230 ºC, as predicted in Figure 10(b) at these high temperatures, Figure 11 (g, h)). On reheating at 1230 ºC the mode grain size (90 μm) and largest grain size (250 μm, which is > SDAS) are markedly larger than those at the lower temperature of 1200 ºC (mode grain size of 75 μm and largest grain size of 205 μm, as seen in Figure 11(f)); the increased proportion of large grains is consistent with the reduced pinning from dissolving Nb-rich precipitates in the interdendritic region, resulting in a weak bimodal grain size distribution that is skewed to a larger size, as seen in Figure 11(h). Abnormal grain growth is still not observed when the interdendritic Nb(C,N) (the most stable particle for the as-cast sample during reheating) starts to dissolve as there is a relatively uniform large grain structure in the dendritic region that can grow into the interdendritic region but then will impinge on large grains from nearby dendritic regions (as the interdendritic regions are relatively narrow). Reheating at 1280 ºC resulted in a uniform coarse grain structure, Figure 11(i, j). No abnormally

large isolated grains were observed in this as-cast steel during all the reheating treatments.

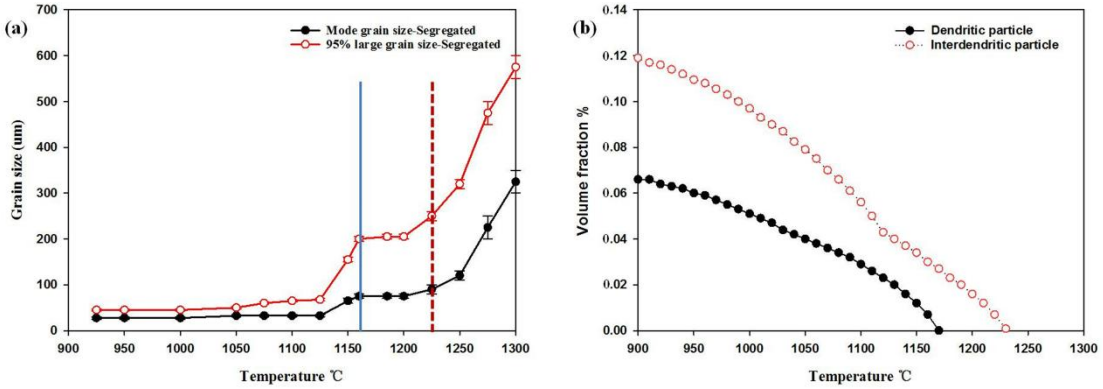

Figure 10 (a) Grain size development with reheat temperatures from 925 ºC to 1300 ºC for the as-cast segregated steel showing the mode grain size and 95% large grain size. The blue solid line indicates the predicted dissolution temperature of the pinning dendritic AlN; and the red dashed line indicates the predicted dissolution temperature of the interdendritic Nb(C,N); (b) predicted precipitate volume fraction in the dendritic and inerdendritic regions against the temperatures.

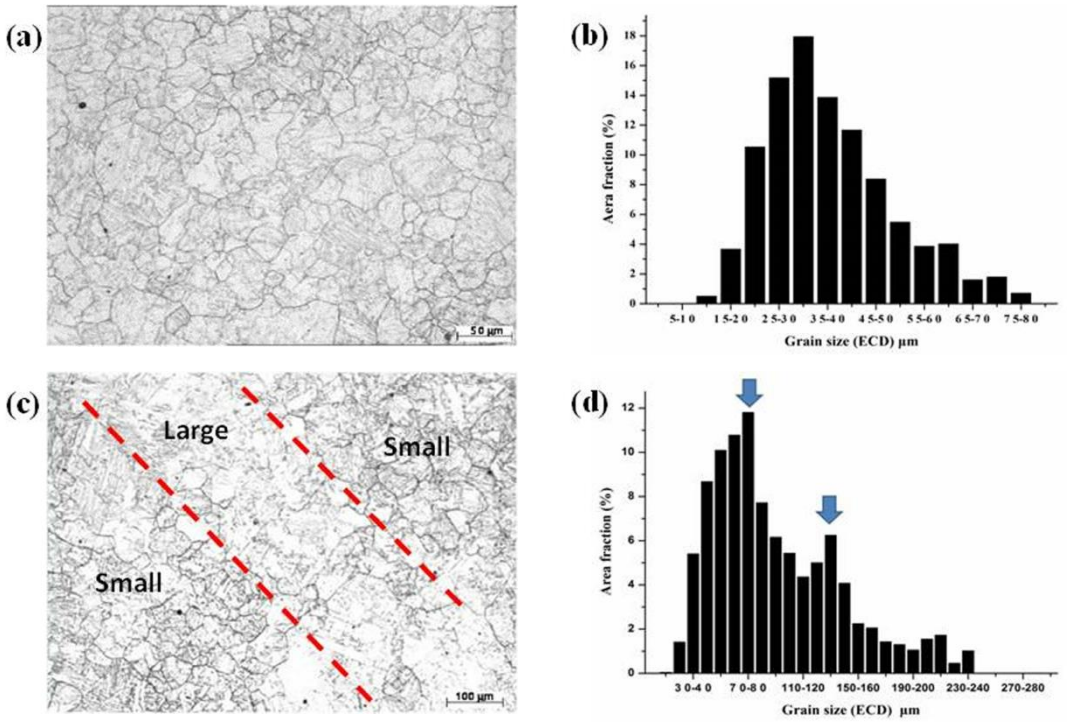

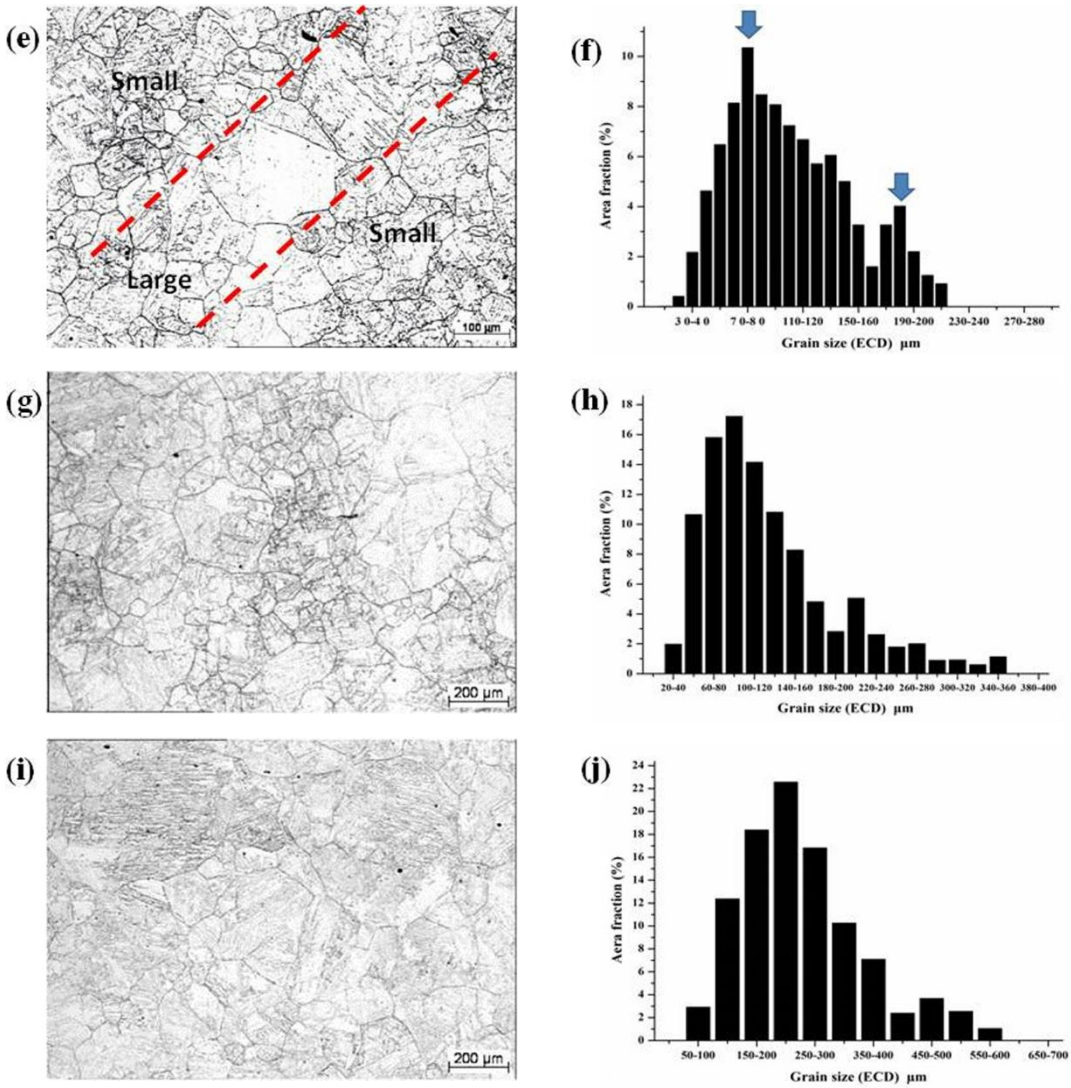

Figure 11 Prior austenite grain structure and grain size distributions for the as-cast segregated steels after reheating for 1 hour at: (a, b) 1130 ºC; (c, d) 1160 ºC; (e, f) 1200 ºC; (g, h) 1230 ºC; and (i, j) 1280 ºC.

SEM was used to characterise the precipitate distribution and any correlation to the occurrence of bimodal grain size development. The micrograph in Figure 12 (a) shows the typical bands of small and large grained regions in the as-cast Al-Nb containing steel reheated to 1160 ºC, where the band separation distance (between two adjacent small grains bands) is similar to the SDAS of around 150 ± 50 μm measured in the initial as-cast microstructure. Coarse Al-rich precipitates (of around 250-300 nm size) with small number density were found in the large grained regions, Figure 12 (c), which indicates that a full dissolution of AlN was not achieved at 1160

ºC (predicted dissolution temperature of dendritic AlN) as being similar to the dissolution behaviour of AlN in the corresponding homogenised steel at 1170 ºC [31]. Spherical Nb-rich particles in clusters were observed in the fine grained regions, as seen in Figure 12 (e). No dendritic Nb-rich particles (in large grained area) or interdendritic Al-rich particles (in fine grained region) were observed at this temperature, which indicates that the predictions for dissolution of these particles are accurate (dissolution temperatures of 1030 ºC for dendritic Nb (C, N) and 1120 ºC for interdendritic AlN). SEM results from samples reheated to 1200 ºC revealed that Nb-rich particles still remained in the fine-grained region but that Al-rich particles were not observed at all, which indicates that the development of a bimodal grain structure in the segregated steels during reheating is consistent with local unpinning in the dendritic regions. Large grain growth in the solute-depleted dendritic regions is caused by the dissolution of Al-rich particles, while the remaining Nb-rich particles in the solute-enriched interdendritic region maintained the finer grain size in this area.

Figure 13 indicates the difference in the prior austenite grain growth under conditions when the pinning Al-rich particles have dissolved for the homogenised [31] and as-cast samples. At reheating temperatures below 1130 ºC, no significant changes in grain size has been observed for the mode grain size (25 - 30 µm) and large (95% accumulated area fraction) grain size (50 – 60 µm) in the homogenised and segregated steel, which indicates that there is a low driving force for grain growth and the inhomogenous precipitates' distribution in the as-cast sample exhibits a similar pinning effect on grain growth compared to the uniformly distributed microalloy-rich particles in the homogenised steel. At a reheating temperature of 1170 ºC (as indicated with the dark dotted line in Figure 13), abnormal grain growth has occurred and resulted in the marked increase in the large grain size in the homogenised steel,

which is due to the local dissolution of AlN. The grain size in the as-cast (segregated condition) sample showed no changes at 1170 ºC compared to that at 1160 ºC, and the grain size was roughly constant with temperature up to 1200 ºC, with a stable mode grain size of around 70 µm and large grain size of about 200 µm; however, the grain size at 1200 ºC in the homogenised steel showed an increase in the mode grain size (above 100 µm) but the large grain size reduced to 200 µm as more uniform grain growth was observed compared to abnormal growth at 1170 ºC. These differences in grain growth behaviour between the homogenised and as-cast steels indicates that segregation resulting in a banded spatial distribution of pinning by microalloy precipitates restricts excessive grain growth from the dendritic region (solute-poor area in the as-cast structure) into the interdendritic region, which limits the development of any potential abnormally large grain structure in the as-cast steel.

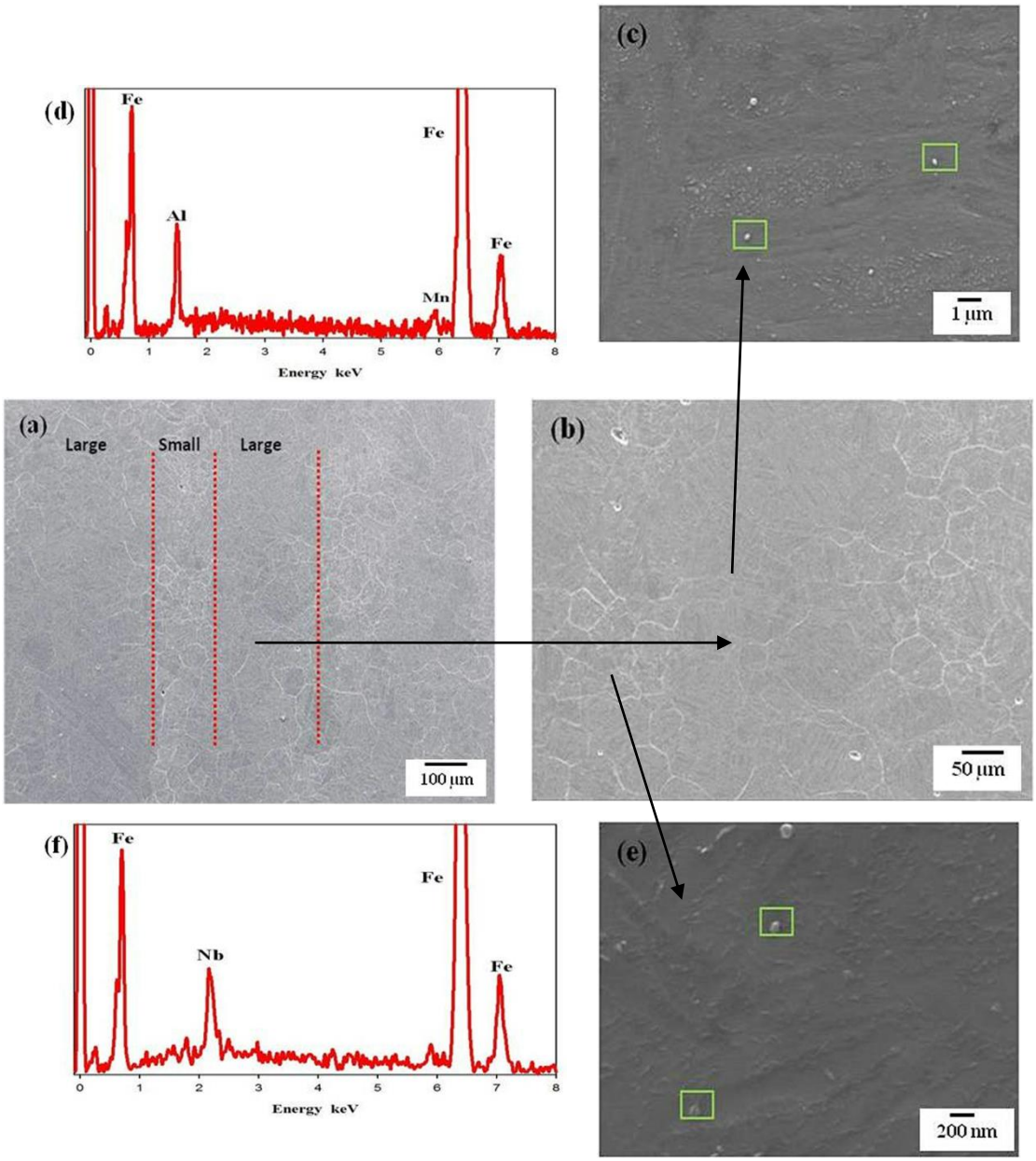

Figure 12 SEM results in segregated samples after reheating at 1160 ºC for 1 hour: (a, b) bands of large and small grains under SEM images; (c) Al-rich particles, expected to be AlN present in the large grain region and (d) EDS trace indicating the Al peak; (e) Nb-rich precipitates, expected to be Nb(C,N) present in small grained region and (f) EDS trace indicating the Nb peak.

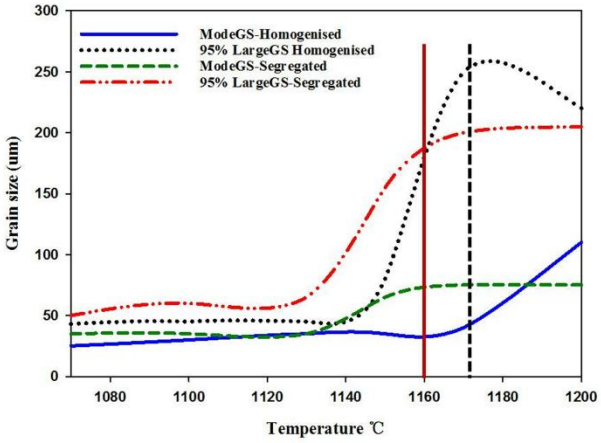

Figure 13 Prior austenite grain growth in homogenised and segregated (as-cast) steels after reheating in the temperature range from 1070 ºC to 1200 ºC. Predicted dissolution temperatures of Al-rich precipitates are indicated as red solid line for 1160 ºC in the dendritic region of the segregated sample, dark dotted line for 1170 ºC in homogenised sample. GS: grain size.

Conclusions

The grain growth behaviour during reheating in an as-cast low carbon Al-Nb steel (containing 0.019 wt% Nb and 0.057 wt% Al) has been investigated and compared to that seen in the same steel when homogenised. In particular the development of non-uniform grain structures related to unpinning caused by dissolution of microalloy precipitates in the cases of uniform precipitate distributions (homogenised steel) and non-uniform distributions (as-cast with solute-rich interdendritic and solute-poor dendritic regions separated by the secondary dendrite arm spacing, SDAS) has been considered. The main conclusions from this work are:

1. Bimodal grain growth occurred in the reheating temperature range from 1160 ºC to 1200 ºC in the as-cast steel due to the dissolution of dendritic AlN, but retention of interdendritic Nb(C,N); the Nb-rich particles in the interdendritic regions play a significant role on grain boundary pinning and hence restricting the growth of large grains originating from the dendritic region. This pinning in the interdendritic regions gives a banded structure of coarse and fine grains and

occurs over a certain temperatures range (e.g. 1160 ºC – 1200 ºC) where the dendritic particles (AlN) have dissolved and until the start of dissolution of the interdendritic Nb-rich particles.

2. No abnormal grain growth resulting in isolated large grains was observed in the as-cast Al-Nb containing steel, whereas abnormal grain growth was observed for the same steel in the homogenised condition. This is because when grain growth occurs by localized dissolution in the dendritic areas of the as-cast steel the large grains are pinned in the interdendritic area limiting the size of these potential abnormally large grains to the segregation distance, i.e. the SDAS.
3. The grain growth behaviour correlated to the pinning effect of microalloying particles and the critical temperatures agree well to the predicted dissolution temperatures for AlN and Nb(C,N) using Thermo-Calc combined with DICTRA simulation for the segregated elemental compositions.

Therefore it is suggested that abnormal grain growth can be avoided in as-cast microalloyed steels if sufficient pinning is provided in the interdendritic regions when grains start to grow in the dendritic regions due to local dissolution of precipitates. The size of the large grains in the bimodal distribution is controlled by the segregation distance (SDAS), which is controlled by the cooling rate through solidification. Thermo-Calc and DICTRA can be used to determine the segregated compositions, microalloy precipitate dissolution temperatures and hence grain structure on reheating if the SDAS is known.

Acknowledgements

The authors would like to thank Tata Steel Europe for the provision of material and the School of Metallurgy and Materials at the University of Birmingham for providing

the facilities required for the research. One of the authors (Fei Wang) is grateful to a departmental scholarship from the School of Metallurgy and Materials as financial support during their PhD.

Disclosure statement

The authors declare that they have no conflicts of interest. Declarations of interest: none.

References

[1] Vervynckt S., Verbeken K., Lopez B., and Jonas J. Modern HSLA steels and role of non-recrystallisation temperature. *Int. Mater. Rev.* **2012**;57(4): 187-207.
[2] Skobir D. A. High-strength low-alloy (HSLA) steels. *Materiali in Tehnologije*. **2011**;45(4): 295-301.
[3] Cuddy L. Microstructures developed during thermomechanical treatment of HSLA steels. *Metall. Trans. A.* **1981**;12(7): 1313-1320.
[4] Rashid M. High-strength, low-alloy steels. *Science*. **1980**;208(4446): 862-869.
[5] Davis C. The effect of microalloy precipitates on final product mechanical properties. *T. Indian I. Metals*. **2006**;59(5): 695-710.
[6] Bhattacharjee D., Davis C., and Knott J. Predictability of Charpy impact toughness in thermomechanically control rolled (TMCR) microalloyed steels. *Ironmak. & steelmak*. **2003**;30(3): 249-255.
[7] Chakrabarti D., Strangwood M., and Davis C. Effect of bimodal grain size distribution on scatter in toughness. *Metall. Mater. Trans. A.* **2009**;40(4): 780-795.
[8] Kundu A., Davis C., and Strangwood M. Grain size distributions after single hit deformation of a segregated, commercial Nb-containing steel: prediction and experiment. *Metall. Mater. Trans. A.* **2011**;42(9): 2794-2806.
[9] Park S. H., Kim S. H., Kim Y. M., and You B. S. Improving mechanical properties of extruded Mg–Al alloy with a bimodal grain structure through alloying addition. *Journal of Alloys & Compounds*. **2015**;646(2): 932-936.
[10] Roy S. Effect of microalloy precipitates on austenite grain growth during reheating treatment of HSLA steel. [PhD]. Indian Institute of Technology, Kharapur, India; 2013.
[11] Wu S. and Davis C. Effect of duplex ferrite grain size distribution on local fracture stresses of Nb-microalloyed steels. *Mater. Sci. Eng.: A.* **2004**;387: 456-460.
[12] Chakrabarti D., Davis C. L., and Strangwood M. Characterisation of bimodal grain structures and their dependence on inhomogeneous precipitate distribution during casting. Mater. Sci. Forum, 2005, Trans Tech Publ, 613-622.
[13] Chakrabarti D., Davis C., and Strangwood M. Characterisation of bimodal grain structures in HSLA steels. *Mater. Charact.* **2007**;58(5): 423-438.
[14] Chakrabarti D. Development of bimodal grain structures and their effect on toughness in HSLA steel. [Ph.D.'s thesis]. University of Birmingham, Birmingham, UK; 2007.
[15] Chakrabarti D., Davis C., and Strangwood M. Development of bimodal grain structures in Nb-containing high-strength low-alloy steels during slab reheating. *Metall. Mater. Trans. A.* **2008**;39(8): 1963-1977.

[16] Chakrabarti D., Davis C., and Strangwood M. The effect of precipitate distributions on HSLA grain structures. International Symposium of Research Students on Material Science and Engineering December, 2004, 20-22.
[17] Zheng S., Davis C., and Strangwood M. Elemental segregation and subsequent precipitation during solidification of continuous cast Nb–V–Ti high-strength low-alloy steels. *Mater. Charact.* **2014**;95: 94-104.
[18] Solecka M., Kopia A., Radziszewska A., and Rutkowski B. Microstructure, microsegregation and nanohardness of CMT clad layers of Ni-base alloy on 16Mo3 steel. *Journal of Alloys & Compounds*. **2018**;751: 86-95.
[19] Cuddy L. J. and Raley J. C. Austenite grain coarsening in microalloyed steels. *Metall. Trans. A.* **1983**;14(10): 1989-1995.
[20] Danon A., Servant C., Alamo A., and Brachet J. Heterogeneous austenite grain growth in 9Cr martensitic steels: influence of the heating rate and the austenitization temperature. *Mater. Sci. Eng.: A*. **2003**;348(1): 122-132.
[21] Enloe C. M., Findley K. O., and Speer J. G. Austenite Grain Growth and Precipitate Evolution in a Carburizing Steel with Combined Niobium and Molybdenum Additions. *Metall. Mater. Trans. A*. **2015**;46(11): 5308-5328.
[22] Flores O. and Martinez L. Abnormal grain growth of austenite in a V–Nb microalloyed steel. *J. Mater. Sci.* **1997**;32(22): 5985-5991.
[23] Karmakar A., Kundu S., Roy S., Neogy S., Srivastava D., and Chakrabarti D. Effect of microalloying elements on austenite grain growth in Nb–Ti and Nb–V steels. *Mater. Sci. Technol.* **2014**;30(6): 653-664.
[24] Rudnizki J., Zeislmair B., Prahl U., and Bleck W. Prediction of abnormal grain growth during high temperature treatment. *Comp. Mater. Sci.* **2010**;49(2): 209-216.
[25] Zhang X. Research on abnormal grain growth in reversely transformed austenite structure. [PhD's thesis]. Hokkaido University, Sanpporo, Hokkaido, Japan; 2014.
[26] Zhang X., Matsuura K., and Ohno M. Abnormal Grain Growth in Austenite Structure Reversely Transformed from Ferrite/Pearlite-Banded Structure. *Metall. Mater. Trans. A.* **2014**;45(10): 4623-4634.
[27] Zhou T. H. and Zurob H. S. Abnormal and post-abnormal austenite grain growth kinetics in Nb–Ti microalloyed steels. *Can. Metall. Quart.* **2011**;50(4): 389-395.
[28] Fernández J., Illescas S., and Guilemany J. Effect of microalloying elements on the austenitic grain growth in a low carbon HSLA steel. *Mater. Lett.* **2007**;61(11): 2389-2392.
[29] Hillert M. On the theory of normal and abnormal grain growth. *Acta Metall.* **1965**;13(3): 227-238.
[30] Manohar P. A., Dunne D. P., Chandra T., and Killmore C. R. Grain Growth Predictions in Microalloyed Steels. *ISIJ Int.* **1996**;36(2): 194-200.
[31] Wang F., Davis C., and Strangwood M. Grain growth behaviour on reheating Al–Nb-containing steel in the homogenised condition. *Materials Science & Technology*. **2018**;34(5): 587-595.
[32] Feng R., Li S., Zhu X., and Ao Q. Microstructural characterization and formation mechanism of abnormal segregation band of hot rolled ferrite/pearlite steel. *Journal of Alloys & Compounds*. **2015**;646: 787-793.
[33] Won Y.-M. and Thomas B. G. Simple model of microsegregation during solidification of steels. *Metall. Mater. Trans. A.* **2001**;32(7): 1755-1767.
[34] Zhang D. Characterisation and modelling of segregation in continuously cast steel slab. [PhD's thesis]. University of Birmingham, Birmingham, UK; 2015.
[35] Zhang D. and Strangwood M. Characterisation and modelling of microsegregation in low carbon continuously cast steel slab. Proceedings of the 2013 International Symposium on Liquid Metal Processing & Casting, 2013, 321-327.
[36] Kundu A. Grain structure development during casting, reheating and deformation of Nb-microalloyed steel. [Ph.D.'s thesis]. University of Birmingham, Birmingham, UK; 2011.